New Mexico Geological Society

Downloaded from: https://nmgs.nmt.edu/publications/guidebooks/55



Gravity and aeromagnetic expression of tectonic and volcanic elements of the southern San Luis Basin, New Mexico and Colorado

V. J. S. Grauch and G. R. Keller
2004, pp. 230-243. https://doi.org/10.56577/FFC-55.230

in:

Geology of the Taos Region, Brister, Brian; Bauer, Paul W.; Read, Adam S.; Lueth, Virgil W.; [eds.], New Mexico Geological Society 55 th Annual Fall Field Conference Guidebook, 440 p. https://doi.org/10.56577/FFC-55

This is one of many related papers that were included in the 2004 NMGS Fall Field Conference Guidebook.

Annual NMGS Fall Field Conference Guidebooks

Every fall since 1950, the New Mexico Geological Society (NMGS) has held an annual Fall Field Conference that explores some region of New Mexico (or surrounding states). Always well attended, these conferences provide a guidebook to participants. Besides detailed road logs, the guidebooks contain many well written, edited, and peer-reviewed geoscience papers. These books have set the national standard for geologic guidebooks and are an essential geologic reference for anyone working in or around New Mexico.

Free Downloads

NMGS has decided to make peer-reviewed papers from our Fall Field Conference guidebooks available for free download. This is in keeping with our mission of promoting interest, research, and cooperation regarding geology in New Mexico. However, guidebook sales represent a significant proportion of our operating budget. Therefore, only *research papers* are available for download. *Road logs*, *mini-papers*, and other selected content are available only in print for recent guidebooks.

Copyright Information

Publications of the New Mexico Geological Society, printed and electronic, are protected by the copyright laws of the United States. No material from the NMGS website, or printed and electronic publications, may be reprinted or redistributed without NMGS permission. Contact us for permission to reprint portions of any of our publications.

One printed copy of any materials from the NMGS website or our print and electronic publications may be made for individual use without our permission. Teachers and students may make unlimited copies for educational use. Any other use of these materials requires explicit permission.

This page is intentionally left blank to maintain order of facing pages.

GRAVITY AND AEROMAGNETIC EXPRESSION OF TECTONIC AND VOLCANIC ELEMENTS OF THE SOUTHERN SAN LUIS BASIN, NEW MEXICO AND COLORADO

V. J. S. GRAUCH[1] AND G. R. KELLER[2]
[1]U. S. Geological Survey, MS 964, Federal Center, Denver, CO 80225, tien@usgs.gov;
[2]University of Texas at El Paso, El Paso, TX 79968, keller@geo.utep.edu

ABSTRACT.—The San Luis Basin has been characterized as an east-tilted, northerly trending rift basin containing a narrow deep graben on the east and a largely buried, intrarift basement horst on the west. We refine these concepts for the southern San Luis Basin by revisiting existing gravity and aeromagnetic data using modern methods. In the New Mexico portion of the basin, the narrow (6-12 km) Taos graben follows a general north-south trend from Costilla near the state line to the Embudo fault at the southern end of the basin. West of the Taos graben, the intrarift basement horst changes orientation from north-south in Colorado to southwestward south of the state line, merging with the Tusas Mountains in a complicated manner that is not entirely understood. At the state line, the Taos graben widens northward to reach 25-30 km wide in the Culebra reentrant in Colorado, accompanied by en echelon stepping of the western graben border to the west. For nearly the entire length of the graben, the gravity-defined western border coincides with Quaternary faults and is followed or paralleled by the course of the Rio Grande. In the southernmost basin, the intrarift horst is absent. Instead, a broad semi-circular gravity low (Tres Orejas gravity low) of ambiguous origin lies west of the geophysically defined Taos graben. Along the southern border of the San Luis Basin, a strong gravity gradient follows the Embudo fault farther westward than previously proposed for a scissors fault configuration. South of the Embudo fault, north-south gradients in both gravity and aeromagnetic data correspond to the Picuris-Pecos fault system and suggest a related, parallel fault exists about 20 km to the west. Prominent circular aeromagnetic anomalies in the Taos Plateau can be associated with individual volcanoes and are used to infer the remanent magnetic polarities the rocks acquired when they cooled. A circular aeromagnetic anomaly near the Gorge bridge suggests a previously unknown volcano lies beneath the Servilleta Basalt. This information can be used to aid future geologic mapping of the Plateau and, in certain circumstances, can help constrain uncertain or multiple age dates for the volcanoes.

INTRODUCTION

The San Luis Basin is a north- to northwest- trending basin that forms a major segment of the northern Rio Grande rift (Fig. 1). It extends for about 200 km across southern Colorado and northern New Mexico and is bordered by the Sangre de Cristo Mountains on the east and the San Juan and Tusas Mountains on the west. Although the valley floor is 30-70 km wide, geophysical data and drilling have established that the deep part of the basin actually occupies a fairly narrow zone (10-30 km wide) adjacent to the Sangre de Cristo mountain front (Keller et al., 1984; Brister and Gries, 1994; Kluth and Schaftenaar, 1994). The narrow zone is bounded on the west by an intrarift basement horst, which is evidenced at the surface by isolated erosional remnants of Oligocene volcanic rocks in the San Luis Hills and Taos Plateau (Lipman and Mehnert, 1979; Thompson et al., 1991). West of the horst in the northern San Luis Basin is a buried, thick section of Eocene through Quaternary sedimentary units and Oligocene volcanic rocks from the San Juan volcanic field that reflect Tertiary history since the late stages of the Laramide orogeny (Brister and Gries, 1994). In the southern San Luis Basin, these subsurface deposits, if present, have been covered by the Pliocene Taos Plateau volcanic field (Fig. 1) and Quaternary alluvial deposits (Lipman and Mehnert, 1979; Dungan et al., 1984).

Because of the extensive alluvial and volcanic cover, gravity and aeromagnetic data were critical tools in developing the original understanding of the geometry of southern San Luis Basin over two decades ago (Kleinkopf et al., 1970; Cordell, 1976a, 1978; Cordell and Keller, 1984; Keller et al., 1984; Cordell et al., 1985). With the advent of color image display, fast computers, and sophisticated geoinformatics tools, we can now re-examine the old data in a new light. We see new details that improve our understanding of the basin geometry and structure, point out possible buried depocenters, and help explain the underlying tectonic controls on the location of the Rio Grande. In addition, the regional aeromagnetic data over the Taos Plateau have never been specifically discussed in the literature even though the data were acquired in 1975 (Kucks et al., 2001). These data provide insight into the nature and lateral extent of individual volcanoes and set the stage for understanding high-resolution aeromagnetic data that have recently been acquired in a much smaller area surrounding the Town of Taos (Grauch et al., 2004).

There are many details yet to be understood about the gravity and aeromagnetic data for the southern San Luis Basin. In this paper, we discuss the gravity and aeromagnetic expression of some of the salient tectonic and volcanic elements within the basin and along its borders. Elements within the basin include the Taos graben, the intrarift horst, Taos Plateau volcanic field, and a poorly understood tectonic feature related to a gravity low in the southernmost basin. Elements of the uplifted rift borders include the Picuris-Pecos and Embudo faults along the southern border and the Latir volcanic field and Questa caldera on the eastern border.

GEOLOGIC SETTING

The southern San Luis Basin, like other parts of the Rio Grande rift, has experienced multiple tectonic events that each have left an imprint on the geology and underlying structure (Keller and Baldridge, 1999). Precambrian events left an underlying suture

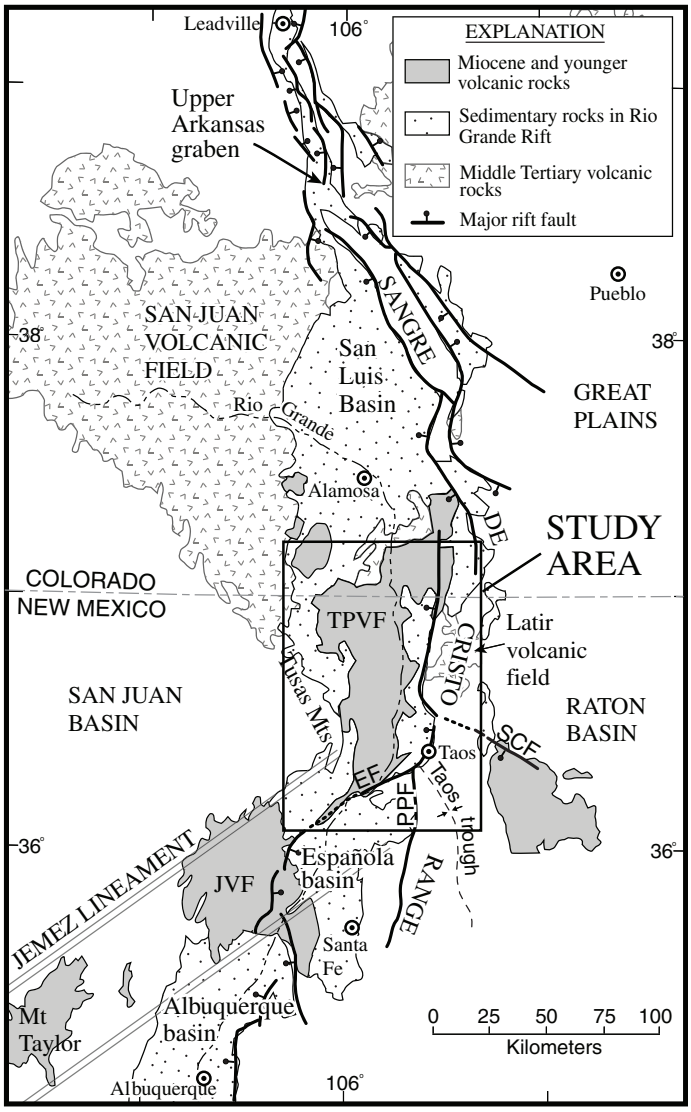


FIGURE 1. Location of the study area within the Rio Grande rift. EF=Embudo fault; JVF=Jemez volcanic field; PPF=Picuris-Pecos fault; SCF=Saladan Creek fault; TPVF=Taos Plateau volcanic field. Geology generalized from Lipman (1983), Baltz and Meyers (1999), and Keller and Baldridge (1999). Jemez lineament from Aldrich (1986).

zone, which passes through the Taos area, manifested as an alignment of Cenozoic magmatic centers along the Jemez lineament (or Jemez zone) (Aldrich, 1986; Keller and Baldridge, 1999; CD-ROM working group, 2002) (Fig. 1). Northeast, north-south, and northwest structural trends of all ages are attributed to pre-existing Precambrian foliations and shear zones (Karlstrom and Humphreys, 1998), and are evident in aeromagnetic anomaly patterns (Cordell and Keller, 1984; Sims et al., 2002).

In Late Paleozoic time, the northwest-trending Uncompahgre-San Luis highlands and Sangre de Cristo uplift were located in the Tusas and Sangre de Cristo Mountains, respectively (Kluth, 1986). Sediments shed from these uplifts filled intervening basins, such as the Taos trough, now present in the southern Taos Range (Fig. 2; Baltz and Myers, 1999). In Laramide time, the Tusas and Sangre de Cristo Mountains were elevated again, shedding sediments that are primarily preserved along the eastern side of the San Juan volcanic field and along the southwestern side of the Tusas Mountains (Fig. 1). From Late Eocene to Late Oligocene time, extensive ash-flow eruptions and lava flows originated from the San Juan volcanic field, blanketing most of the surrounding area. The Latir volcanic field (Fig. 1), which includes the 25.7 Ma Questa caldera (Meyer and Foland, 1991; Fig. 2), formed in the southern San Luis Basin during the waning stages of this activity, immediately prior to the inception of the Rio Grande rift (Lipman et al., 1986).

Early rifting was generally characterized by broad, relatively shallow basins developed under an extensional regime that was oriented northeast-southwest (Morgan et al., 1986). In the southern San Luis Basin, early rifting (26-25 Ma) was accompanied by the development of northwest-striking faults in the Tusas Mountains, basaltic magmatism, and deposition of volcaniclastic sediments (Lipman, 1983; Lipman et al., 1986; Thompson et al., 1991). By middle to late Miocene (15-8 Ma), the extension direction had changed orientation to east-west and rifting became characterized by high-angle faulting, graben formation, and volcanism in the nearby Jemez volcanic field (Morgan et al., 1986; Ingersoll et al., 1990).

Accumulation of Santa Fe Group sediments in the southern San Luis Basin was well underway by 18 Ma (Ingersoll et al., 1990; Bauer and Kelson, 2004). At that time, the eastern border of the Taos graben may have followed the Sangre de Cristo range front without interruption from the state line to the Picuris-Pecos fault zone in the Picuris Mountains (Fig. 1; Bauer and Kelson, 2004). Sometime after 18 Ma, the Embudo fault zone developed and became linked with the Sangre de Cristo fault system to form the Taos embayment (Bauer and Kelson, 2004). The Embudo fault zone aligns with the Jemez lineament (Fig. 1) and is theorized to transfer strain between the east-tilted San Luis and west-tilted Española basins (Muehlberger, 1979; Faulds and Varga, 1998).

In late Miocene-Pliocene time (6 to 2 Ma), volcanism of the Taos Plateau volcanic field (Fig. 1) was characterized by multiple eruptions of basaltic- and intermediate-composition magma from scattered cones and shield volcanoes. During the middle and late stages of volcanic activity, a geochemically unique suite of olivine tholeiitic basalt flows spread over the area, (Servilleta Basalt of Lipman and Mehnert, 1979; Dungan et al., 1984). Although collectively the Servilleta Basalt is laterally extensive, individual flows are commonly discontinuous, interfingered, and interbedded with sediments of variable thickness (Dungan et al., 1984).

Basin tilting and uplift of surrounding rift borders continued into Quaternary time, resulting in the accumulation of coalescing alluvial fans near the eastern mountain fronts and incision of the Rio Grande gorge (Dungan et al., 1984; Heffern, 1990). Quaternary fault activity was concentrated at the Sangre de Cristo and Embudo faults, and in swarms of north-south-striking faults cutting alluvial deposits within the Taos graben (Los Cordovas, Sunshine Valley, and Mesita faults on Fig. 2; Machette and Personius, 1984; Kelson et al., 2004).

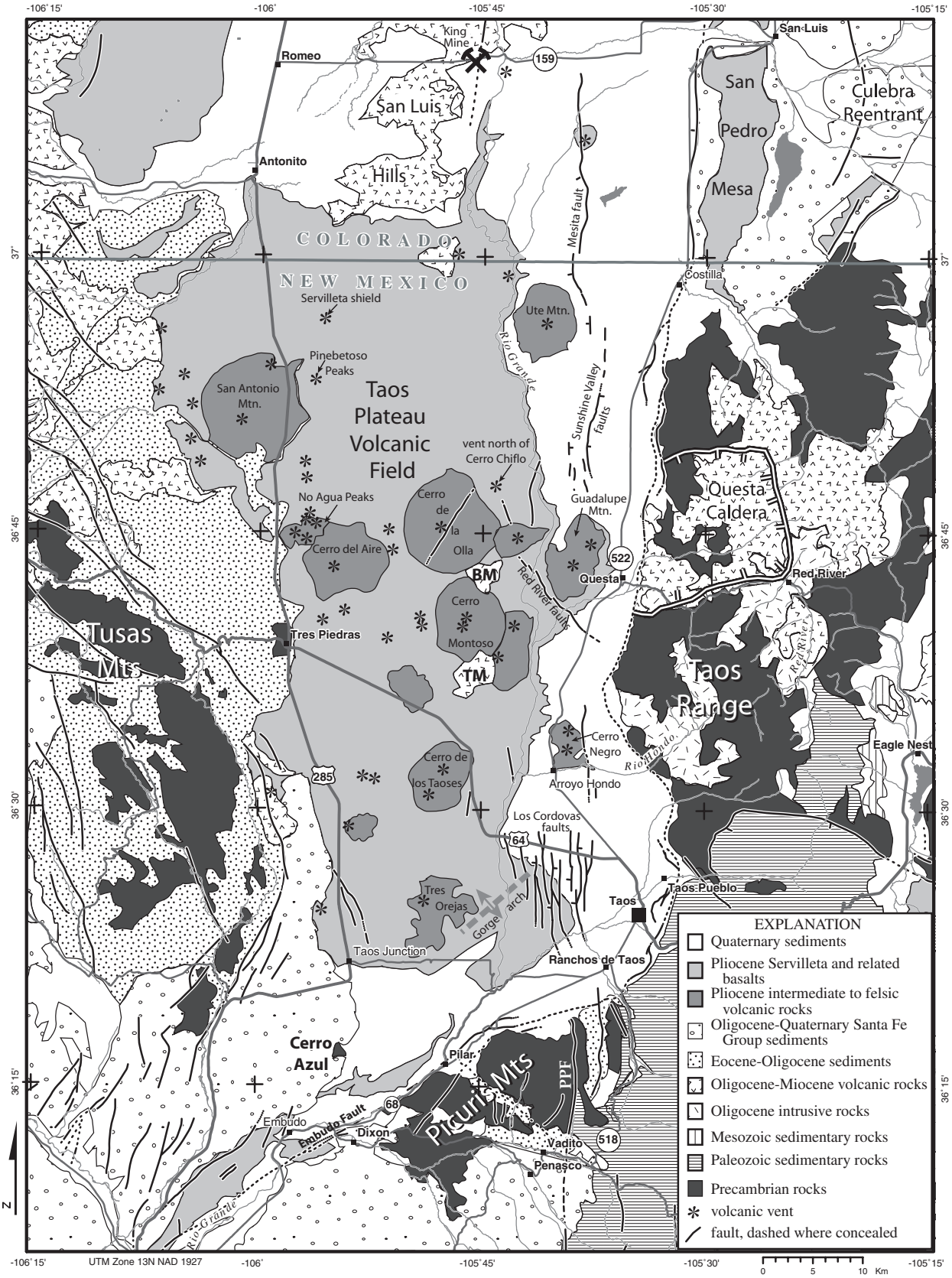


FIGURE 2. Geology of the study area highly generalized from New Mexico Bureau of Geology and Mineral Resources (2003) and Green (1992). Volcanic vents are from R. Thompson (USGS, written communication, 2004). Gorge arch and faults within the basin in New Mexico are from Machette and Personius (1984). Questa caldera outline from Lipman and Reed (1989). BM=Brushy Mountain; TM=Timber Mountain; PPF=Picuris-Pecos fault.

GRAVITY DATA

Gravity studies focus on subtle variations in the Earth's gravitational field that are due to changes in bulk density relative to an average density (2.67 g/cm^3) of the crust. Gravity data are particularly effective in determining the subsurface configuration of the basins within the Rio Grande rift due to the generally large contrast in density between the low-density basin fill and the moderate- to high-density bedrock composing the basin floor and sides. In addition, gravity data can be used to locate basement uplifts and major structures, and to estimate thickness of basin fill.

Typically, gravity data collected at specific locations in the field are processed as Bouguer gravity anomaly data or Bouguer gravity data. This data reduction (Hildenbrand et al., 2002) includes subtraction of theoretical or predicted values for the Earth's gravitational attraction at the elevation of the measurement point, removal of the effects of homogeneous masses underneath, and correction for the effects of topographic masses. In order to focus on density variations within the upper crust, a regional field is commonly removed from Bouguer gravity data. Subtraction of a regional field based on an isostatic model of topography, which results in an isostatic residual gravity map, is a common way to examine density variations in the upper crust (Simpson et al., 1986).

Groups conducting gravity studies in the Rio Grande rift and adjacent areas have had a long history of cooperation by sharing data and coordinating efforts to fill in areas of sparse coverage. These efforts have resulted in a large collection of gravity data, upon which subsequent efforts continually build. For this study, we obtained recent versions of this database by extracting the data in grid form from a recent compilation for New Mexico that extends 15 minutes of latitude northward into Colorado (Kucks et al., 2001). Station coverage is adequate for a regional study (averaging 2-5 km apart over most of the study area) except for a large (15 x 15 km) area in the Sangre de Cristo Mountains east of Taos (Kucks et al, 2001). A more recently updated database for this area includes additional stations and is available from the internet (<http://paces.geo.utep.edu>), but the additional data do not substantially fill in this regional gap. The data shown in Plate 3 were extracted from the 1-km-interval grid of the New Mexico isostatic residual gravity data (Kucks et al., 2001) and reprojected to Universal Transverse Mercatur (UTM zone 13, North American Datum 1927).

AEROMAGNETIC DATA

Aeromagnetic surveys measure variations in the strength of the Earth's magnetic field that are produced by changes in total magnetization of the rocks in the crust. Total magnetization is the vector sum of the induced and remanent magnetizations. The induced component is determined by the quantity and type of magnetic minerals (commonly titanomagnetites), measured as magnetic susceptibility. The remanent component is based on the permanent alignment of magnetic domains within magnetic minerals and is measured using paleomagnetic methods (Butler, 1992). Igneous and crystalline metamorphic rocks commonly have high total magnetizations compared to other rock types, whereas sedimentary rocks and poorly consolidated sediments have much lower magnetizations (Reynolds et al., 1990; Hudson et al., 1999). In addition, total magnetizations of volcanic rocks are commonly dominated by the remanent component (Reynolds et al., 1990). Thus, volcanic rocks can produce high-amplitude positive or negative aeromagnetic anomalies, depending on whether the rocks formed during a period of normal or reversed polarity of the Earth's magnetic field.

The aeromagnetic data for this study (Plate 4) were combined from pre-existing 500-m-interval grids compiled for Colorado and New Mexico (Oshetski and Kucks, 2000; Kucks et al., 2001). As part of the compilation process, data from disparate surveys were analytically continued to a common observation surface 304 m (1,000 ft) above ground and digitally merged. Although this provides a consistent database, the quality of the data are highly dependent on the original flight parameters. Data for New Mexico came from surveys that were flown at different levels (averaging 304 m or 1,000 ft above ground) with lines spaced 1.6 km (1 mi) apart. These surveys give good definition of anomaly shapes in map view but poor resolution of low-amplitude signal. Data for Colorado came from one survey flown at 122 m (400 ft) above ground with lines spaced 3.2 km (2 mi) apart. This survey resolves low-amplitude signal along individual flight lines but has poor anomaly definition. The poor quality of the Colorado data is evident from its choppy appearance (Plate 4).

Data from two small aeromagnetic surveys in New Mexico have not been included in the aeromagnetic map for reasons of convenience. Their inclusion would not alter conclusions at the regional scale of this study. One was flown over the Latir volcanic field and discussed in detail previously (Cordell, 1976b; Moss and Abrams, 1985). The other was flown recently around the Town of Taos (pink outline on Plate 5) and is discussed elsewhere in this volume (Grauch et al., 2004).

The aeromagnetic grids from the two state compilations were reprojected to Universal Transverse Mercatur (UTM zone 13, North American Datum 1927) using a 1-km grid interval, digitally merged, then transformed by a standard reduction-to-pole operation to correct for shifts of the main anomaly from the center of the magnetic source (Blakely, 1995). To do this transformation, we assume that the total magnetizations of most rocks in the study area align parallel or anti-parallel to the Earth's main field (declination=10^o, inclination=64^o). The collinearity assumption probably works well for the Tertiary volcanic rocks. Its validity for older rocks is unknown, but would be problematic only if remanent magnetization is predominant.

EXPRESSION OF BASIN GEOMETRY

In this section we review the geophysical expression of key elements of rift basin geometry of the southern San Luis Basin. These elements include the Taos graben, the intrarift horst, and a tectonic feature of ambiguous origin related to a large gravity low (Tres Orejas gravity low) in the southernmost portion of the basin.

The variability of density that is now recognized in the underlying Precambrian basement rocks (Treviño et al., 2004) imparts ambiguity to interpretation of gravity highs and lows. To compensate, we focus the discussion on the locations of steep gravity gradients (gravity gradient lines) to define rift-graben borders (Cordell, 1979; Cordell et al., 1985) and use simple basin models (Keller et al., 1984) only to illustrate three-dimensional basin geometry. For this report, steep gravity gradients were located by finding the maximum slopes of best-fit planes within a 10 x 10 km moving window across the data grid, following the method of Grauch and Johnston (2002). The technique is similar to that of Cordell (1979), except that the moving window focuses on regional gradients spanning 10 km rather than the more local gradients spanning only the neighboring grid points (a window width of 3 x 3 km). As a consequence, the gravity gradient lines of Plate 3 show the same general geometry of the Taos graben as obtained earlier (Cordell and Keller, 1984; the Taos-Questa graben of Cordell et al., 1985), but the lines are somewhat straighter and more continuous.

Taos Graben

Previous workers have long recognized the prominent, elongate gravity low associated with the Taos graben in the southern San Luis Basin (Plate 3; Cordell, 1978; Cordell and Keller, 1984; Keller et al, 1984; Cordell et al., 1985). The gravity gradient lines indicate a remarkably narrow (6-12 km wide) graben from 17 km north of Questa to the latitude of Taos (Fig. 3 and Plate 3). The eastern, gravity-defined border generally follows the poorly exposed Sangre de Cristo fault zone along the range front (Fig. 3; Machette and Personius, 1984) from Costilla south to a point where the range front makes a sharp jog to the southeast near the latitude of Timber Mountain (TM on Fig. 2 and Plate 3). South of this point, the gravity-defined border diverges significantly from the large embayment in the range front (Fig. 3), crossing west of the town of Taos and marking the western edge of a complicated series of structural benches that step down into the basin away from the mountain front (the Town Yard bench of Bauer and Kelson, 2004). Recently flown high-resolution aeromagnetic data also show these basement blocks (Grauch et al., 2004; Plate 5). The blocks lack expression in the lower resolution regional aeromagnetic data (pink outline on Plate 4).

The western border of the Taos graben is delineated by a gravity gradient line extending from 17 km north of Questa to the latitude of Tres Orejas (Figs. 2, 3, and Plate 3; Cordell, 1978; Cordell and Keller, 1984; Cordell et al., 1985). It is informally called the Gorge fault (Bauer and Kelson, 2004) owing to its general coincidence with the extent of the Rio Grande gorge, where the river has carved a deep canyon through the basalts of the Taos Plateau. South of Arroyo Hondo, the gravity gradient marking the Gorge fault flattens (Plate 3), indicating that the bedrock/basin-fill interface at the graben border deepens to the south. South of where the gravity gradient line ends, the aeromagnetic data show a gradient corresponding to an abrupt shift from generally higher values on the west to generally lower values on the east that follows the linear extension of the western graben border to the south (short-dashed line west of Taos on Plate 4). The aeromagnetic gradient could be due to juxtaposition of magnetically different volcanic rocks within the basin, the basement, or both. Its coincidence with the southern extension of the Gorge fault is compelling evidence that this expression is produced by an underlying fault of unknown age.

Keller et al. (1984) estimated 2,000-3,000 m of basin fill (Fig. 4) and depths from 3,000 to more than 5,000 m to Precambrian basement within the Taos graben. The estimates were derived from two separate gravity models: one that assumed a density contrast of 350 kg/m^3 between basin fill and adjacent rocks, and the other a contrast of 250 kg/m^3 between Precambrian basement and all younger rocks (including pre-rift Tertiary rocks). Given that the composition and densities of rocks underlying the southern San Luis Basin remain largely unknown, we have not attempted to improve these estimates. Lipman and Mehnert (1979) used estimated depths of 5-6 km to Precambrian basement west of Questa caldera (Keller et al., 1984) and 2 km of maximum topographic relief in the adjacent mountains to infer 7 to 8 km of total displacement along the Sangre de Cristo fault.

South to north past Questa, both gravity-defined Taos graben borders appear to make a parallel bend to the northeast (Plate 3), ultimately shifting the graben by 5 km to the east. The bend orients the graben in a northeast-southwest direction for a short section near Questa. The Rio Grande gorge makes the same bend where it is nearly coincident with the western graben border (Gorge fault) along this section (Figs. 2 and 3). The river follows the graben border rather than the northwest-striking, down-to-the-northeast Red River fault zone, which crosses this section obliquely. This evidence for an underlying tectonic control of the river suggests that previous discussions of the development of the Rio Grande gorge, which assume the Red River fault zone is the only locus of structural deformation in the area (e.g., Heffern, 1990), should be re-evaluated.

North of Questa, the gravity gradient line defining the Gorge fault appears to die out 5 km south of Ute Mountain. However, the trend of the gravity contours can be followed north-northwest through Ute Mountain to join the north-south portion of a gravity gradient line that we informally name the Olla-King gravity gradient (Plate 3). This gravity gradient defines the eastern boundary fault of the intrarift horst and is so named because it trends northeast across Cerro de la Olla parallel to a northeast-striking fault, then gradually veers to the north to pass near the King Mine in Colorado (Figs. 2 and 3). One can interpret the relations of the gravity gradients near Ute Mountain to represent a series of stepped, en echelon faults (not shown) that transfer normal offset from the Gorge fault on the south to the fault represented by the Olla-King gravity gradient on the north. A decrease of offset at the north end of the Gorge fault helps explain why north-south Quaternary faults that align across the state line (Figs. 2 and 3; the Sunshine Valley and Mesita faults of Machette and Personius, 1984) switch from down-to-the-east where they coincide with the Gorge fault in New Mexico to down-to-the-west farther north in Colorado. In addition, the Rio Grande gradually migrates to the west as one follows it headward from the Gorge fault on the south to the Olla-King gravity gradient on the north (Figs. 2 and 3), suggesting that the graben borders have been an underlying struc-

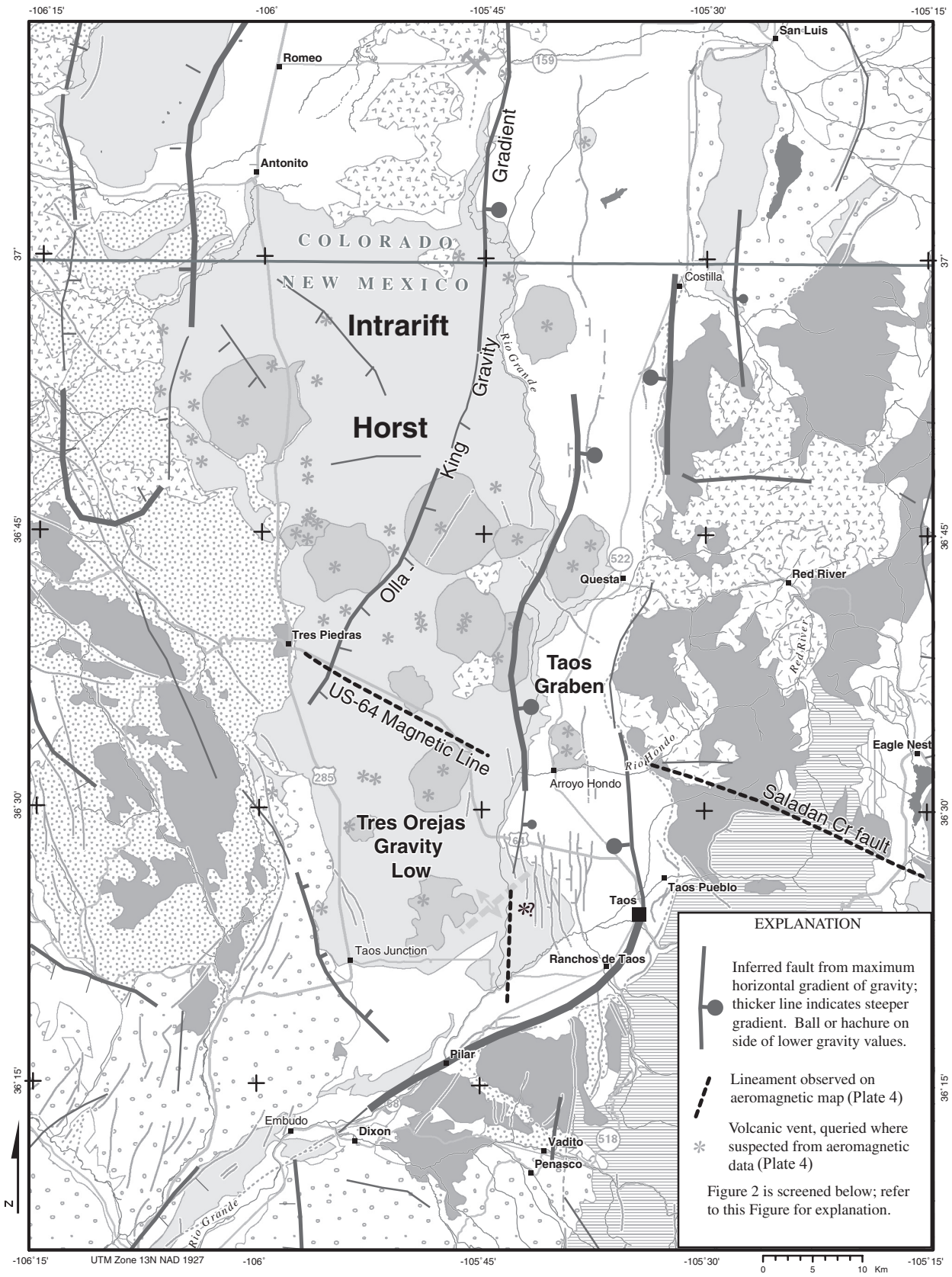


FIGURE 3. Screened version of the generalized geology of Figure 2 overlain with geophysically interpreted features. These features are also overlain on regional gravity (Plate 3) and aeromagnetic data (Plate 4) for comparison. See text for discussion of their origin and significance.

tural control on the development of the river from the San Luis Hills on the north to almost as far as Pilar on the south.

The eastern border of the Taos graben is not geophysically apparent north of the state line, where the range front opens into the Culebra reentrant (Figs. 2, 3, and Plate 3). Here the Sangre de Cristo fault system follows the western side of San Pedro Mesa (Machette and Personius, 1984), but the main rift margin lies 5-8 km to the east within a complexly faulted zone that has net down-to-the-southwest displacement (Wallace, 1995). Between this rift margin and the Olla-King gravity gradient, the graben is about 25-30 km wide (Fig. 3).

Tres Orejas Gravity Low

In the extreme southwestern portion of the San Luis Basin, a semi-circular gravity low, which we informally call the Tres Orejas gravity low (Plate 3), is located west of the southern extension of the Taos graben. Assuming a density contrast of 350 kg/m^3 between adjacent bedrock and basin fill, Keller et al. (1984) estimated that 1,000-3,000 m of low-density rocks (presumably basin fill) are contained within the area of the low (Fig. 4).

The Tres Orejas gravity low could represent a Tertiary early rift basin, a Late Paleozoic sedimentary basin, or a combination of these. A broad, early rift basin is generally supported by several congruent geophysical and geologic inferences. High-amplitude, positive aeromagnetic anomalies northeast of a magnetic lineament that generally follows highway US-64 (US-64 magnetic line on Fig. 3) appear to broaden and become more subdued to the southwest (Plate 4). Early to Middle Tertiary (35-22 Ma) intermediate-composition volcanic rocks are thought to underlie the area of high-amplitude positive anomalies (Lipman and Mehnert, 1979; Thompson et al., 1986) and are likely magnetic sources. The change in aeromagnetic character to the southwest of the US-64 magnetic lineament suggests that the magnetic sources dip moderately to steeply to the south or southwest, in contrast to the overlying Servilleta Basalt flows, which dip gently to the southeast (Dungan et al., 1984). The inferred southerly dip originating from a northwest-trending hinge at the US-64 magnetic lineament and the broadness of the gravity low are suggestive of an early rift basin. One possible scenario is that the gravity low represents a basin floored by Eocene to Oligocene volcanic rocks that subsided during Late Oligocene time. A depocenter here at this time might explain where sediments shed from the rapid uplift of the San Luis Hills at ~26 Ma (Thompson et al., 1991) were deposited and why these sediments are largely missing in outcrop (R. Thompson, oral commun., 2004).

Alternatively, Baltz and Myers (1999) argue that the Tres Orejas gravity low (although they didn't name it) reflects thick Pennsylvanian and Permian sedimentary rocks (as much as 1800 m or 6000 ft) related to the Late Paleozoic Taos trough. This scenario requires that the Picuris-Pecos fault did not form the western boundary of the Taos trough during Ancestral Rockies time as is commonly depicted by others in the literature (e.g., Woodward et al., 1999) and that there has been no appreciable post-Paleozoic lateral movement on the fault. The magnetically expressed Saladan Creek fault, which formed the northern boundary of the Taos trough (Baltz and Myers, 1999), generally aligns with the northern boundary of the Tres Orejas gravity low along the US-64 magnetic lineament. This alignment suggests a similar, underlying structural control, despite their very different geophysical expressions.

Intrarift Horst

Remnants of Middle Tertiary (22-25 Ma) intermediate-composition volcanic rocks at Brushy Mountain and Timber Mountain (Fig. 2) have commonly been used as evidence for the intrarift, Precambrian basement horst under the Taos Plateau (e.g., Lipman and Mehnert, 1979). Although the basal portions of these eruptive sequences are not exposed, the rocks have been conjectured to lie directly on Precambrian basement, as do other rocks of this age in the surrounding mountains (Lipman et al., 1986; Thompson et al., 1986; Thompson et al., 1991). This geologic evidence, in conjunction with the gravity gradient line (Olla-King gradient line on Plate 3; Cordell et al., 1985), supports the existence of the horst north of the latitude of Arroyo Hondo. The Tres Orejas gravity low provides evidence that the intrarift horst does not continue south of Arroyo Hondo, as discussed in the previous section.

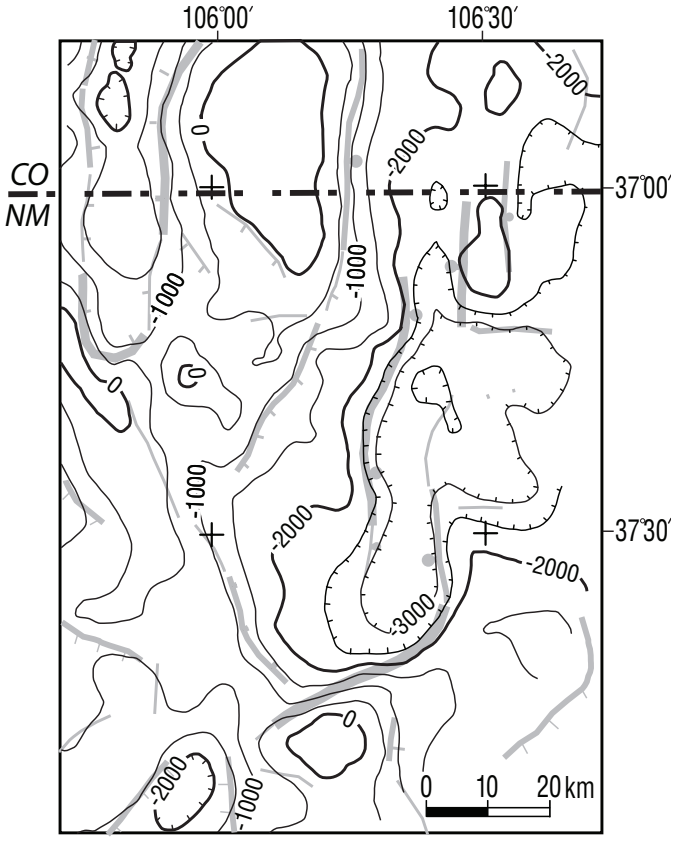


FIGURE 4. Contours of estimated depth (meters) to the base of basin fill extracted for the study area from the gravity model of Keller et al. (1984). A density contrast of 350 kg/m^3 was assumed between the fill and adjacent rocks. Contour interval= 500 m. Five wells north of the study area were used for model calibration. Faults inferred from gravity gradients (thick gray lines) are from Plate 3.

Color maps of the gravity data call attention to markedly lower gravity values (-12-8 mgal) over the inferred horst in the vicinity of Brushy and Timber Mountains compared to those (8-24 mgal) over the horst in the area of the western San Luis Hills (Plate 3). The area of lower gravity values is generally triangular, bounded by the Olla-King gravity gradient, the US-64 magnetic lineament, and the Gorge fault (Plate 3). Gravity models suggest that 1,000-2,000 m of low-density basin fill is present in this area (Fig. 4; Keller et al., 1984), in apparent contradiction to the standard geologic concept of uplifted Precambrian basement directly overlain by Oligocene through Pliocene volcanic rocks.

There are several plausible explanations for the apparent discrepancy between the geologic and gravity evidence related to (1) differences in density of the basement rocks, (2) a down-dropped structural bench that was covered by sediments and/or volcanic rocks before 25 Ma, (3) underlying sedimentary rocks from the Taos trough that were offset along the Picuris-Pecos fault after the Late Paleozoic, or (4) a buried extension of the Questa caldera or underlying batholith. The model of Keller et al. (1984; Fig. 4) supports the second explanation primarily as a consequence of the simplifying assumptions. We cannot rule out any of these explanations. However, considering the concentration of volcanic vents in this area (Plate 3), the extent of strong positive magnetic anomalies generally limited to the area and *not* present in the Questa caldera (Plate 4), and the linearity to the boundaries of the area, our preference is the second explanation. If this explanation is correct, it suggests that a thick section (1,000-2,000 m or more) of volcanic rocks and/or sediments older than 25 Ma underlie this triangular area.

EXPRESSION OF FAULTS IN THE SOUTHERN BORDER AREA

The San Luis Basin is bounded on the south by the northeast-striking Embudo fault zone (Figs. 1 and 2), which has been commonly described as a scissors-like transfer zone that developed since Pliocene time (Muehlberger, 1979; Manley, 1984). In this model, the pivot point is thought to lie between Embudo and Pilar, on a northwest-trending basement saddle that is evident in the gravity data underlying Precambrian exposures at Cerro Azul (Plate 3; Cordell, 1979). More recent studies (Kelson et al., 2004) describe the Embudo fault zone northeast of Pilar as a complex system of left-oblique, northwest-down, strike-slip fault strands, which developed sometime during Miocene time. The strong gravity gradient along the Embudo fault, which continues partway across the basement saddle, suggests that large vertical displacement along the fault continues from Pilar to Dixon and does not decrease to near zero until reaching as far west as Embudo (Fig. 4 and Plate 3).

Immediately south of the Embudo fault zone, both the gravity and the aeromagnetic data generally show a 20-km-wide block of high values that is bounded on the east by the Picuris-Pecos fault system and on the west by a parallel gradient in both data sets (Plates 4 and 6). Although the gradients bounding the magnetic block are more linear than those bounding the gravity block, both blocks are generally elongate north-south and extend south of the study area into the Santa Fe Range (Kucks et al., 2001). The northern boundary of the gravity-high block follows the Embudo fault. The northern boundary of the magnetic block follows a high-amplitude east-northeast-trending magnetic high that parallels the Embudo fault zone but is displaced to the south by almost 10 km (Plate 4). This magnetic "ridge" follows the trends of Proterozoic foliation and shear zones in the Picuris Mountains (Karlstrom and Daniel, 1993; Bauer and Ralser, 1995; Williams et al., 1999). However, the stratigraphic and structural complexity in this area (Williams et al., 1999) makes it difficult to ascertain which unit(s) are the magnetic source(s). Between the magnetic "ridge" and the mountain front, the aeromagnetic expression over the exposed Precambrian rocks is featureless, indicating a different rock type than that to the south. This weakly magnetic but dense Precambrian basement near Pilar may continue northward, under the southern San Luis Basin.

The aeromagnetic gradient along the western side of the geophysically defined 20-km wide block discussed above is probably caused by an intra-basement fault. Gravity and seismic-reflection models across the northern Española basin (Cordell, 1979; Ferguson et al., 1995) show only gradual westward dip on the basement, suggesting that a major fault here would be restricted to basement rocks and was not active during the development of the Española basin. A pre-rift strike-slip fault, such as the hypothetical Tusas-Picuris fault of Karlstrom and Daniel (1993), is a plausible explanation.

On the eastern side of the 20-km wide block, the gravity gradient following the Picuris-Pecos fault system is gradual and probably corresponds to basement relief related to the neighboring Taos trough (Fig. 2). In contrast, the aeromagnetic gradient is sharp, reflecting the juxtaposition of highly magnetic rocks on the west against very weakly magnetic rocks on the east that produce a low, featureless area (Plate 4). The juxtaposition can be explained by 37 km of right-lateral offset recognized from the displacement of Precambrian strata along the fault (summarized in Bauer and Ralser, 1995). The history of movement on this fault is still under debate (Cather, 1999; Lucas et al., 2000; Woodward, 2000; E. Erslev, Colorado State University, oral commun., 2004).

The prominent difference in basement magnetic anomalies juxtaposed and offset a known amount along the Picuris-Pecos fault inspired Cordell and Keller (1984) to "palinspastically restore" the aeromagnetic map along this and other north-south gradients in northern New Mexico. The intent of the exercise, using more detailed data than that used in an earlier demonstration (Chapin, 1983), was to speculate on how much north-south lateral displacement of Precambrian basement blocks has occurred during Phanerozoic tectonic events. These "restored" patterns of aeromagnetic anomalies remain intriguing, but a thorough investigation of their sources is required to resolve the ambiguities in interpreting them. Identical aeromagnetic anomalies can be produced by rocks of different ages, and aligning anomalies using a simple lateral offset does not account for the complications arising from uplift, erosion, thrusting, and extensional faulting that clearly have occurred in the region since Precambrian time.

EXPRESSION OF VOLCANIC FIELDS

In this section, we compare the gravity and aeromagnetic expressions of the Latir volcanic field, which surrounds and includes the Questa caldera (Fig. 2), and the Taos Plateau volcanic field. The Latir field is characterized by overall low gravity values and aeromagnetic highs of moderate magnitude (Plates 4 and 6). In contrast, the Taos Plateau is characterized by many high-amplitude (either positive or negative) aeromagnetic anomalies and a gravity expression that cannot be distinguished from the underlying graben structure.

Latir Volcanic Field and Questa Caldera

The aeromagnetic expression of rocks related to the Latir volcanic field is indistinguishable from that of the country rock (Plate 4). The patterns of the anomalies primarily reflect the form of topography, which is typical for crystalline rocks in areas of rugged terrain (Grauch, 1987), and individual anomalies correspond to a variety of rock types, including volcanic rocks, plutons, and Precambrian basement (Cordell, 1976b; Moss and Abrams, 1985).

The Questa caldera is not readily apparent in the aeromagnetic data except along its southern margin (Plate 4). The featureless aeromagnetic character in this area is probably related to mineralized, hydrothermally altered intrusions that are aligned east-west along the caldera margin (Lipman, 1983; Moss and Abrams, 1985; Lipman et al., 1986). The caldera is more evident in the gravity data, where it generally corresponds to the lowest part of a gravity low that extends over much of the Taos Range between Taos Pueblo and San Luis (Plate 3). Preliminary interpretations attributed the source of the regional gravity low to a large batholith under the Questa caldera (Lipman, 1983). Detailed gravity and electrical geophysical studies later determined that the Questa batholith is likely concentrated in a narrow (10-km wide), north-south zone centered on longitude 105°30'W and extending from the caldera on the north to the latitude of Arroyo Hondo on the south (Cordell et al., 1985). The more regional extent of low gravity values may be caused by rootless Precambrian basement thrust over less dense sedimentary rocks (Cordell and Keller, 1984; Treviño et al., 2004).

A west-northwest-trending alignment of aeromagnetic highs generally corresponds to intrusions along the southern margin of the Latir volcanic field that straddle the Rio Hondo (Fig. 3), but also extends much further to the southeast (Plate 4). The Rio Hondo pluton (generally north of Rio Hondo) is the likely source of the string of aeromagnetic anomalies because it corresponds spatially to individual anomalies better than does the younger Lucero Peak pluton located nearby (Moss and Abrams, 1985). The Rio Hondo pluton was emplaced 26-25 Ma along a northwest-striking fault (Lipman, 1983), which is probably related to the Saladan Creek fault that Baltz and Myers (1999) consider as the northern boundary of Taos trough (Fig. 2). Lipman (1983) regarded this fault and the numerous northwest-trending dikes that cross-cut the Rio Hondo pluton as evidence for a northeast-southwest extension direction during early rifting. However, the more westerly trend of the aeromagnetic alignment that follows the Late Paleozoic Saladan Creek fault suggests that magma followed a much older fault at depth during early rifting. Similarly, the north-south elongation of the geophysically delimited Questa batholith north of the Saladan Creek fault may indicate that preexisting faults guided the magma at depth (Cordell et al., 1985).

The western side of the Questa caldera is cut by the Sangre de Cristo rift-related range front fault (Lipman and Reed, 1989). Whether the caldera and underlying intrusions are present west of the range within the Taos graben is unknown. In conceptual models, geologists are mixed in showing a limited (Lipman, 1983; Meyer and Foland, 1991) or a far-reaching (Baltz and Myers, 1999) western extent. The available geophysical data do not resolve the question (Cordell et al., 1985; Plates 4 and 6).

Taos Plateau Volcanic Field

Unlike the moderate- to low-amplitude positive aeromagnetic anomalies characteristic of the Latir volcanic field, the anomalies over the Taos Plateau have generally high amplitudes, are both positive and negative, and commonly show circular or elongated shapes (Plate 4). The circular anomalies generally have good correspondence to vents (pink asterisks on Plate 4), strongly suggesting that the aeromagnetic anomalies are a reflection of the shape and lateral extent of the underlying volcanoes. The Servilleta Basalt (away from vent areas) probably does not include sufficient lateral magnetic contrast to produce high-amplitude aeromagnetic anomalies because of the layer-like morphology and generally low remanent magnetization compared to other rock types (1 A/m compared to >10 A/m; Brown et al., 1993).

The relative petrologic uniformity of individual volcanoes (Lipman and Mehnert, 1979) and the high amplitudes of the anomalies suggest that the remanent polarities of volcanoes in the Taos Plateau field can be inferred where corresponding aeromagnetic anomalies have good correlation with the form of topography (Grauch, 1987). Good examples include Ute and San Antonio Mountains (Fig. 2), where the lateral extents of the aeromagnetic anomalies have excellent correlation with the shapes of the volcanic edifices (compare Plates 1 and 6). The correlation is positive (both have similar shape) at San Antonio Mountain and negative (the anomaly shape is the opposite of the terrain shape) at Ute Mountain, indicating that the rocks carry strong remanent magnetization with normal polarity at San Antonio Mountain and reversed polarity at Ute Mountain. Polarities inferred this way agree with measured remanent polarities (Brown et al., 1993) at four volcanoes where paleomagnetic sample sites can be matched to aeromagnetic anomalies (Cerro Negro, San Antonio Mountain, the northern side of Cerro de los Taoses, and the southwestern side of Guadalupe Mountain; Fig. 5). Excellent correspondence between measured and inferred polarities was also found at the Pliocene Cerros del Rio volcanic field (Hudson et al., 2004; Grauch et al., in press), which is located at the southern end of the Española basin (Fig. 1).

Because volcanic activity at the Taos Plateau spans four million years and many reversals of the Earth's magnetic field (Fig. 5), aeromagnetic and paleomagnetic data are most useful when

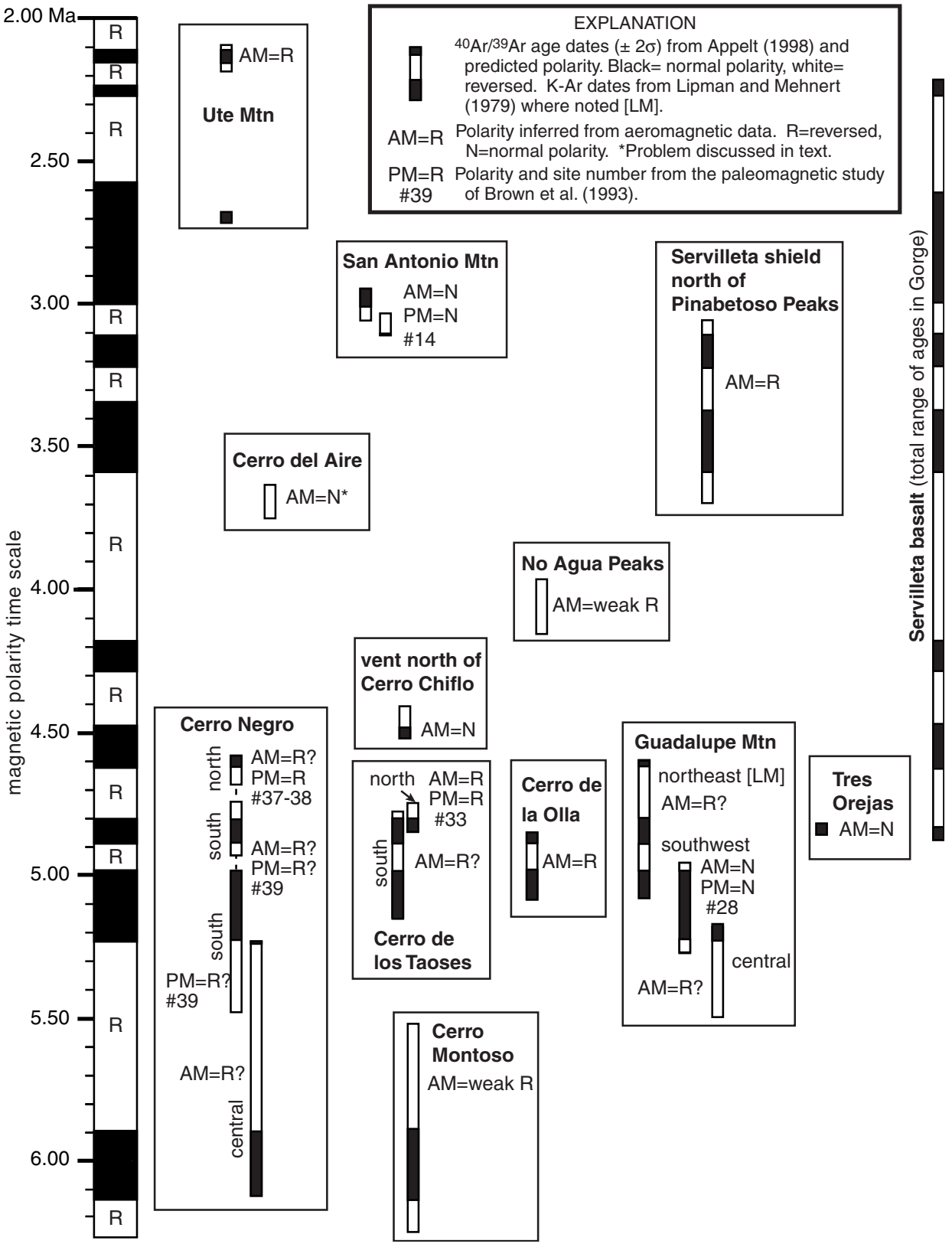


FIGURE 5. Magnetic polarities inferred from aeromagnetic data and measured from a paleomagnetic study (Brown et al., 1993) compared to those predicted by age for selected volcanoes. Polarities predicted from established magnetic polarity time scales (Berggren et al., 1995; Honey et al., 1998) and $^{40}Ar/^{39}Ar$ (Appelt, 1998) and K-Ar (as noted by Lipman and Mehnert, 1979) radiometric age dates. Age ranges are shown for two standard deviations (± 2σ). Age-polarity comparisons are separated by geographic location (Fig. 2) where differences are apparent. Inferred polarities are queried where age comparison is uncertain. No polarity comparisons are available for Servilleta basalt (see text).

combined with age data. In Figure 5, we use published $^{40}Ar/^{39}Ar$ and K-Ar radiometric ages (Lipman and Mehnert, 1979; Appelt, 1998) to predict the polarities associated with various volcanoes from established magnetic polarity time scales (Berggren et al., 1995; Honey et al., 1998). These predicted polarities are then compared to those inferred from aeromagnetic maps (Plate 4) and those measured from paleomagnetic samples (Brown et al., 1993). As in the studies of the Cerros del Rio volcanic field (Thompson et al., 2002; Hudson et al., 2004), these comparisons can be used in conjunction with the aeromagnetic map and paleomagnetic sampling as guides to locating contacts between similar-looking basalts that have different magnetic polarities.

When aeromagnetic-terrain correlations are carefully considered, the age-polarity comparisons can help constrain uncertain age data and resolve multiple age dates as well as serve as a geologic mapping tool. For example, the normal polarity inferred for the vent north of Cerro Chiflo (Fig. 2) suggests that its actual age falls within the time of normal rather than reversed polarity (an age range of 4.48-4.52 Ma rather than 4.41-4.52 Ma; Fig. 5). Similarly, the reversed polarity inferred for Cerro de la Olla (Fig. 2) narrows the age range from 4.85-5.09 Ma to 4.89-4.98 Ma (Fig. 5). By similar reasoning, the most recent eruptive activity probably occurred during reversed polarity intervals at Ute Mountain (2.09-2.11 or 2.15-2.17 Ma) and at the northern vents of Cerro de los Taoses (4.74-4.80 Ma), and during normal polarity intervals at San Antonio Mountain (2.94-3.04 Ma) and the southwestern vent of Guadalupe Mountain (4.98-5.23 Ma; Fig. 5). Negative aeromagnetic values surrounding the positive anomaly at San Antonio Mountain and negative values surrounding the positive anomaly at Ute Mountain (Plate 4) may reflect rocks from the earlier eruptive episodes of opposite polarity (Fig. 5).

Where circular anomalies are not centered over volcanic edifices, the anomalies are likely produced by an underlying, older volcano that constitutes the largest volume of material underneath the vent area. The more recent flows may be only a thin cover on the surface (Hudson et al., 2004). Underlying sources are suspected on the northeast side of Guadalupe Mountain and on the southern sides of Cerro Negro and Cerro de los Taoses, and are indicated by uncertain age-polarity associations (Fig. 5).

The polarity-age comparisons also point out places where further study is required. For example, the reversed polarity expected for the age date from a single sample at Cerro del Aire does not match the normal polarity inferred from aeromagnetic data (Fig. 5). This mismatch presently cannot be explained.

A circular negative magnetic anomaly about 2 km in diameter is located within a larger area of negative magnetic values along the east side of the Rio Grande gorge 8 km west of Taos (queried asterisk on Plate 4). This area is cut by numerous, north-south-striking faults (Los Cordovas faults of Machette and Personius, 1984; Fig. 2). The similarity to circular negative anomalies associated with volcanic vents elsewhere allow us to speculate that the source is a volcano with reversed polarity remanence. Preliminary inspection of profiles crossing the anomaly (not shown) suggests an approximate depth of about 900 m (3000 ft). Alternatively, the circular shape may arise from poor aeromagnetic resolution of negative anomalies associated with angular fault blocks cut by both north- and northeast-striking faults. Northeast-striking faults in this area are suggested by the northeast orientation of the axis of the Gorge arch (Fig. 2), a local warping defined by asymmetric stream channels (Muehlberger, 1979), and by northeast-striking linear gradients parallel to Rio Pueblo de Taos found in high-resolution aeromagnetic data just to the east (pink outline on Plate 4; Grauch et al., 2004). Additional collection of high-resolution aeromagnetic data over the postulated vent may resolve this question.

Despite excellent stratigraphic exposure of multiple Servilleta Basalt flows within the Rio Grande gorge (Dungan et al., 1984), attempts to relate remanent polarities from paleomagnetic measurements to magnetic polarity time scales have suffered from problematic dating techniques (Brown et al., 1993). More recently, Appelt (1998) dated samples from localities similar in description to the paleomagnetic study (Brown et al., 1993), but did not provide enough information for direct comparison. We show the maximum age range and associated multiple polarity events for comparison only (Fig. 5).

CONCLUSIONS

The San Luis Basin has been characterized as an east-tilted rift basin containing a narrow deep graben on the east and an intrarift basement horst on the west. This view comes primarily from evidence in the Colorado portion of the San Luis Basin, where the basin geometry is evident from extensive subsurface drilling, seismic data, and a number of rock outcrops. The Pliocene Taos Plateau volcanic field covers much of the southern San Luis Basin. A rift basin geometry similar to the north has been inferred to underlie this area based primarily on gravity data and scant geologic evidence, in concepts developed over two decades ago. In this paper, we re-rexamine the existing gravity and aeromagnetic data for the southern San Luis Basin to better understand the tectonic and volcanic elements that are expressed. As a result, we see details that improve broad concepts of basin geometry developed earlier and that raise important questions about the composition and structure of the underlying rocks. We also present new observations on the aeromagnetic expression of the Taos Plateau that have not been discussed before. Our main conclusions follow.

1. Gravity data indicate that the concept of a narrow graben on the east and a basement horst on the west that is well understood for the northern San Luis Basin can only be loosely applied to the southern part of the basin. South of the state line, the north-south intrarift horst evident in Colorado bends southwestward and merges with the Tusas Mountains in a complicated manner. The narrow (6-12 km) Taos graben, as defined by parallel gravity gradients, can be followed in a general north-south orientation from 17 km north of Questa to the latitude of Arroyo Hondo. The western graben border follows the Rio Grande gorge (Gorge fault); the eastern border follows the Sangre de Cristo range front fault system. In the southernmost part of the basin, the presence of the semi-circular Tres Orejas gravity low, despite its uncertain origin, indicates the intrarift horst is absent. Continuation of the Taos graben into this part of the basin is suggested by an aero-

magnetic gradient on the west and by a major gravity gradient that strikes north-south across the Taos embayment on the east.

2. From south to north of Ute Mountain near the state line, the gravity-defined western graben border steps westward from a location that is coincident with the Quaternary Sunshine Valley faults to the eastern boundary of the intrarift horst in the southern San Luis Hills. The Rio Grande makes a similar, albeit more transitional, realignment, suggesting an underlying tectonic control. The westward step of the graben border coincides with the widening of the basin to about 25-30 km in the Culebra reentrant in southern Colorado.

3. The intrarift horst corresponds to high gravity values except in the vicinity of Brushy and Timber Mountains, where exposed middle Tertiary volcanic rocks are commonly used as evidence of the horst. In this location, the lower gravity values can be explained in a number of ways involving variations in density, structural relief, or both. Although none of these can be ruled out, we prefer an explanation that entails a down-dropped structural bench related to the intrarift horst that was covered by sediments and/or volcanic rocks before 25 Ma.

4. On the uplifted southern border of the San Luis Basin, both gravity and aeromagnetic data generally show a 20-km wide block of high values. The block is bounded on the east by gradients related to the well known Picuris-Pecos strike-slip fault system, and on the west by parallel, north-south gradients possibly related to another strike-slip fault, which predated rifting. The gravity block is bounded on the north by a strong gravity gradient that coincides with the Embudo fault, which marks the southern border of the San Luis Basin. The persistence of the gravity gradient westward to Embudo suggests that large vertical displacement on this fault occurs farther west than previous hypotheses suggest.

5. Circular aeromagnetic anomalies in the Taos Plateau correspond well to the locations of volcanic vents. Normal or reversed polarity remanence was inferred for individual volcanoes (Fig. 5), based on whether corresponding aeromagnetic anomalies were positive or negative, respectively. Inspection of aeromagnetic anomalies in comparison to terrain shape suggests that some of the anomalies are produced by buried sources, presumably related to earlier eruptions. A circular negative aeromagnetic anomaly near the Gorge bridge suggests a previously unknown volcano lies beneath Servilleta Basalt.

6. The aeromagnetic interpretations can be used, especially in conjunction with acquisition of higher resolution aeromagnetic data and new paleomagnetic samples, to aid future geologic mapping of similar-looking basalts. Comparing the remanent polarities inferred from aeromagnetic data to existing age dates shows that the inferred polarities can help constrain uncertain or multiple age dates under certain circumstances.

ACKNOWLEDGMENTS

This paper has benefited greatly from discussions with Ren Thompson, Paul Bauer, and Brian Brister and reviews by Mark Hudson, Viki Bankey, and Chuck Chapin.

REFERENCES CITED

Aldrich, M.J., Jr., 1986, Tectonics of the Jemez lineament in the Jemez Mountains and Rio Grande Rift: Journal of Geophysical Research, v. 91, p. 1753-1762.

Appelt, R.M., 1998, 40Ar/39Ar geochronology and volcanic evolution of the Taos Plateau volcanic field, northern New Mexico and southern Colorado [MS thesis], New Mexico Institute of Mining and Technology, Socorro, NM.

Baltz, E.H., and Myers, D.A., 1999, Stratigraphic framework of upper Paleozoic rocks, southeastern Sangre de Cristo Mountains, New Mexico, with a section on speculations and implications for regional interpretation of Ancestral Rocky Mountain paleotectonics: New Mexico Bureau of Mines and Mineral Resources Memoir 48, 269 pp.

Bauer, P.W., and Kelson, K.I., 2004, Cenozoic structural development of the Taos area, New Mexico: New Mexico Geological Society, 55th Field Conferenc Guidebook, p. 129-146.

Bauer, P.W., and Ralser, S., 1995, The Picuris-Pecos fault--repeatedly reactivated, from Proterozoic(?) to Neogene: New Mexico Geological Society, 46th Field Conference, Guidebook, p. 111-115.

Berggren, W.A., Kent, D.V., Swisher, C.C., III, and Aubry, M.P., 1995, A revised Cenozoic geochronology and chronostratigraphy, *in* Berggren, W.A., Kent, D.V., Aubry, M.P., and Hardenbol, J., eds., Geochronology, time scales and global stratigraphic correlation: Society of Sedimentary Geologists Special Publication 54, p. 129-212.

Blakely, R.J., 1995, Potential theory in gravity and magnetic applications: Cambridge University Press 441 pp.

Brister, B.S., and Gries, R.R., 1994, Tertiary stratigraphy and tectonic develoment of the Alamosa basin (northern San Luis Basin), Rio Grande rift, south-central Colorado, *in* Keller, G.R., and Cather, S.M., eds., Basins of the Rio Grande rift: Structure, stratigraphy, and tectonic setting, Geological Society of America Special Paper 291, p. 39-58.

Brown, L.L., Caffall, N.M., and Golombek, M.P., 1993, Paleomagnetism and tectonic interpretations of the Taos Plateau volcanic field, Rio Grande rift, New Mexico: Journal of Geophysical Research, v. 98, p. 22,401-22,413.

Butler, R.F., 1992, Paleomagnetism: Magnetic domains to geologic terranes: Boston, Blackwell Scientific, 319 p.

Cather, S.M., 1999, Implications of Jurassic, Cretaceous, and Proterozoic piercing lines for Laramide oblique-slip faulting in New Mexico and rotation of the Colorado Plateau: Geological Society of America, v. 111, p. 849-868.

CD-ROM working group, 2002, Structure and evolution of the lithosphere beneath the Rocky Mountains: Initial results from the CD-ROM experiment: GSA Today, v. 12, no. 3, p. 4-10.

Chapin, C.E., 1983, An overview of Laramide wrench faulting in the southern Rocky Mountains with emphasis on petroleum exploration, *in* Lowell, J.D., and Gries, Robbie, ed., Rocky Mountain foreland basins and uplifts: Denver, CO, Rocky Mountain Associate of Geologists, p. 169-179.

Cordell, L., 1976a, Aeromagnetic and gravity studies of the Rio Grande graben in New Mexico between Belen and Pilar: New Mexico Geological Society Special Publication 6, p. 62-70.

Cordell, L., 1976b, Aeromagnetic map of the Wheeler-Latir-Costilla section of the Sangre de Cristo Mountains in New Mexico: New Mexico Geological Society, 27th Field Conference, Guidebook , p. 281-282.

Cordell, L., 1978, Regional geophysical setting of the Rio Grande rift: Geological Society of America Bulletin, v. 89, p. 1073-1090.

Cordell, L., 1979, Gravimetric expression of graben faulting in Santa Fe country and the Española Basin, New Mexico: New Mexico Geological Society, 30th Field Conference, Guidebook, p. 59-64.

Cordell, L., and Keller, G.R., 1984, Regional structural trends inferred from gravity and aeromagnetic data in the New Mexico-Colorado border region: New Mexico Geological Society, 35th Field Conference, Guidebook, p. 21-23.

Cordell, L., Long, C.L., and Jones, D.W., 1985, Geophysical expression of the batholith beneath Questa caldera, New Mexico: Journal of Geophysical Research, v. 90, p. 11,263-11,269.

Dungan, M.A., Muehlberger, W.R., Leininger, L., Peterson, C., McMillan, N.J., Gunn, G., Lindstrom, M., and Haskin, L., 1984, Volcanic and sedimentary stratigraphy of the Rio Grande gorge and the Late Cenozoic geologic evolution of the southern San Luis valley: New Mexico Geological Society 35th Field Conference, Guidebook, p. 157-170.

Faulds, J.E., and Varga, R.J., 1998, The role of accommodation zones and transfer zones in the regional segmentation of extended terranes, *in* Faulds, J.E.,

and Stewart, J.H., eds., Accommodation Zones and Transfer Zones: The Regional Segmentation of the Basin and Range Province: Boulder, CO, Geological Society of America Special Paper 323, p. 1-45.

Ferguson, J.F., Baldridge, W.S., Braile, L.W., Biehler, S., Gilpin, B., and Jiracek, G.R., 1995, Structure of the Española basin, Rio Grande rift, New Mexico, from SAGE seismic and gravity data: New Mexico Geological Society 46th Field Conference, Guidebook, p. 105-110.

Grauch, V.J.S., 1987, A new variable-magnetization terrain correction method for aeromagnetic data: Geophysics, v. 52, p. 94-107.

Grauch, V.J.S., Bauer, P.W., and Kelson, K.I., 2004, Preliminary interpretation of high-resolution aeromagnetic data collected near Taos, New Mexico: New Mexico Geological Society, 55th Field Conference, Guidebook, p. 244-256.

Grauch, V.J.S., and Johnston, C.S., 2002, Gradient window method: A simple way to separate regional from local horizontal gradients in gridded potential-field data: 72nd Annual International Meeting, Society of Exploration Geophysicists, Expanded Abstracts, CD-ROM.

Grauch, V.J.S., Sawyer, D.A., Hudson, M.R., Minor, S.A., and Thompson, R.A., in press, Chapter D: Gravity and aeromagnetic studies, *in* Minor, S.A., ed., The Cerrillos Uplift, the La Bajada Constriction, and Hydrogeologic Framework of the Santo Domingo Basin, Rio Grande Rift, New Mexico, U. S. Geological Survey Professional Paper.

Green, G.N., 1992, The digital geologic map of Colorado in ARC/INFO format, version 1.0: U. S. Geological Survey Open-file Report 92-0507, http://pubs.usgs.gov/of/1992/ofr-92-0507/

Heffern, E.L., 1990, A geologic overview of the Wild Rivers Recreation Area, New Mexico: New Mexico Geological Society, 41st Field Conference, Guidebook, p. 229-236.

Hildenbrand, T.G., Briesacher, A., Flanagan, G., Hinze, W.J., Hittelman, A.M., Keller, G.R., Kucks, R.P., Plouff, D., Roest, W.R., Seeley, J., Smith, D.A., and Webring, M., 2002, Rationale and operational plan to upgrade the U.S. gravity database: U. S. Geological Survey Open-file Report 02-463, 14 pp.

Honey, J.G., Hudson, M.R., and Obradovich, J.D., 1998, The occurrence of the Reunion II subchron in lacustrine beds in the Beaver Basin, Utah, *in* Tomida, Y., Flynn, L.J., and Jacbos, L.L., eds., Advances in Vertebrate Paleontology and Geochronology: Tokyo National Science Museum Monograph 14, p. 17-38.

Hudson, M.R., Mikolas, M., Geissman, J.W., and Allen, B., 1999, Paleomagnetic and rock magnetic properties of Santa Fe group sediments in the 98th Street core hole and correlative surface exposures, Albuquerque Basin, New Mexico: New Mexico Geological Society, 50th Field Conference, Guidebook, p. 355-362.

Hudson, M.R., Thompson, R.A., Barbá, K.E., Grauch, V.J.S., Sawyer, D.A., and Warren, R.G., 2004, Paleomagnetism as a link between geologic and aeromagnetic mapping of the Cerros del Rio volcanic field, Rio Grande rift, New Mexico: U. S. Geological Survey Open-file Report 2004-1093, p. 31.

Ingersoll, R.V., Cavazza, W., Baldridge, W.S., and Shafiqullah, M., 1990, Cenozoic sedimentation and paleotectonics of north-central New Mexico: Implications for initiation and evolution of the Rio Grande rift: Geological Society of America Bulletin, v. 102, p. 1280-1296.

Karlstrom, K.E., and Daniel, C.G., 1993, Restoration of Laramide right-lateral strike slip in northern New Mexico by using Proterozoic piercing points: Tectonic implications from the Proterozoic to the Cenozoic: Geology, v. 21, p. 1139-1142.

Karlstrom, K.E., and Humphreys, E.D., 1998, Persistent influence of Proterozoic accretionary boundaries in the tectonic evolution of southwestern North America: Interaction of cratonic grain and mantle modification events: Rocky Mountain Geology, v. 33, p. 161-179.

Keller, G.R., and Baldridge, W.S., 1999, The Rio Grande rift: A geological and geophysical overview: Rocky Mountain Geology, v. 34, p. 121-130.

Keller, G.R., Cordell, L., Davis, G.H., Peeples, W.J., and White, G., 1984, A geophysical study of the San Luis Basin: New Mexico Geological Society, 35th Field Conference, Guidebook, p. 51-57.

Kelson, K.I., Bauer, P.W., Unruh, J.R., and Bott, J.D.J., 2004, Late Quaternary characteristics of the northern Embudo fault, Taos County, New Mexico: New Mexico Geological Society, 55th Field Conference, Guidebook, p. 147-157.

Kleinkopf, M.D., Peterson, D.L., and Johnson, R.B., 1970, Reconnaissance geophysical studies of the Trinidad quadrangle, south-central Colorado: U.S. Geological Survey Professional Paper 700-B, p. 78-85.

Kluth, C.F., 1986, Plate tectonics of the Ancestral Rocky Mountains, *in* Peterson, J.A., ed., Paleotectonics and sedimentation: AAPG Memoir 41: Tulsa, OK, American Association of Petroleum Geologists, p. 353-369.

Kluth, C.F., and Schaftenaar, C.H., 1994, Depth and geometry of the northern Rio Grande rift in the San Luis Basin, south-central Colorado, *in* Keller, G.R., and Cather, S.M., eds., Basins of the Rio Grande Rift: Structure, Stratigraphy, and Tectonic Setting: Boulder, Colorado, Geological Society of America Special Paper 291, p. 27-37.

Kucks, R.P., Hill, P.L., and Heywood, C.E., 2001, New Mexico aeromagnetic and gravity maps and data: A web site for distribution of data, version 1.0: U. S. Geological Survey Open-File Report 01-0061, http://pubs.usgs.gov/of/2001/ofr-01-0061/

Lipman, P.W., 1983, The Miocene Questa caldera, northern New Mexico: Relation to batholith emplacement and associated molybdenum mineralization, The Genesis of Rocky Mountain Ore Deposits: Changes with time and tectonics: Proceedings of the Denver Region Exploration Geologists Society Symposium, p. 133-149.

Lipman, P.W., and Mehnert, H.H., 1979, The Taos Plateau volcanic field, northern Rio Grande rift, New Mexico, *in* Riecker, R.E., ed., Rio Grande Rift: Tectonics and Magmatism: Washington, D.C., American Geophysical Union, p. 289-311.

Lipman, P.W., Mehnert, H.H., and Naeser, C.W., 1986, Evolution of the Latir volcanic field, northern New Mexico, and its relation to the Rio Grande rift, as indicated by Potassium-argon and fission track dating: Journal of Geophysical Research, v. 91, p. 6329-6345.

Lipman, P.W., and Reed, J.C., Jr., 1989, Geologic Map of the Latir Volcanic Field and Adjacent Areas, Northern New Mexico: U. S. Geological Survey, 1:48000

Lucas, S.G., Anderson, O.J., and Black, B.A., 2000, Implications of Jurassic, Cretaceous, and Proterozoic piercing lines for Laramide oblique-slip faulting in New Mexico and rotation of the Colorado Plateau: Discussion: Geological Society of America Bulletin, v. 112, p. 789-795.

Machette, M.N., and Personius, S.F., 1984, Map of Quaternary and Pliocene faults in the eastern part of the Aztec 1° x 2° quadrangle and the western part of the Raton 1° x 2° quadrangle, northern New Mexico, U. S. Geological Survey Miscellaneous Field Studies Map MF-1465-A, scale 1:250000.

Manley, K., 1984, First-day road log from Taos to Embudo, Dixon, Peñasco, Vadito, Tres Ritos, Holman Hill, and back to Taos via U.S. Hill and Talpa: New Mexico Geological Society, 35th Field Conference, Guidebook, p. 303-319.

Meyer, J., and Foland, K.A., 1991, Magmatic-tectonic interaction during early Rio Grande rift extension at Questa, New Mexico: Geological Society of America Bulletin, v. 103, p. 993-1006.

Morgan, P., Seager, W.R., and Golombek, M.P., 1986, Cenozoic thermal, mechanical and tectonic evolution of the Rio Grande rift: Journal of Geophysical Research, v. 91, p. 6263-6276.

Moss, C.K., and Abrams, G.A., 1985, Aeromagnetic maps of the Latir Peak and Wheeler Peak wildernesses and the Columbine-Hondo wilderness study area, Taos County, New Mexico: U. S. Geological Survey, 1:50,000

Muehlberger, W.R., 1979, The Embudo fault between Pilar and Arroyo Hondo, New Mexico: An active intracontinental transform fault: New Mexico Geological Society, 30th Field Conference, Guidebook , p. 77-82.

New Mexico Bureau of Geology and Mineral Resources, 2003, Geologic Map of New Mexico, 1:500,000, New Mexico Bureau of Geology and Mineral Resources.

Oshetski, K.C., and Kucks, R.P., 2000, Colorado aeromagnetic and gravity maps and data: A web site for distribution of data: U. S. Geological Survey Open-File Report 00-0042, <http://pubs.usgs.gov/of/2000/ofr-00-0042/colorado.htm>.

Reynolds, R.L., Rosenbaum, J.G., Hudson, M.R., and Fishman, N.S., 1990, Rock magnetism, the distribution of magnetic minerals in the Earth's crust, and aeromagnetic anomalies: U. S. Geological Survey Bulletin 1924, 24-45 pp.

Simpson, R.W., Jachens, R.C., Blakely, R.J., and Saltus, R.W., 1986, A new isostatic residual gravity map of the conterminous United States with a discussion on the significance of isostatic residual anomalies: Journal of Geophysical Research, v. 91, p. 8348-8372.

Sims, P.K., Stein, H.J., and Finn, C.A., 2002, New Mexico structural zone--an analogue of the Colorado mineral belt: Ore Geology Reviews, v. 21, p. 211-225.

Thompson, R., Grauch, V.J.S., Sawyer, D., and Hudson, M.R., 2002, Aeromagnetic expression of volcanic rocks of the Cerros Del Rio volcanic field, Rio

Grande rift, north-central New Mexico: GSA Abstracts with Programs, v. 34, p. 451-452.

Thompson, R.A., Dungan, M.A., and Lipman, P.W., 1986, Multiple differentiation processes in early-rift calc-alkaline volcanics, northern Rio Grande rift, New Mexico: Journal of Geophysical Research, v. 91, p. 6046-6058.

Thompson, R.A., Johnson, C.M., and Mehnert, H.H., 1991, Oligocene basaltic volcanism of the northern Rio Grande rift: San Luis Hills, Colorado: Journal of Geophysical Research, v. 96, p. 13,577-13,592.

Treviño, L., Keller, G.R., Andronicos, C.L., and Quezada, O., 2004, Rootless mountains and gravity lows in the Sangre de Cristo Mountains, southern Colorado-northern New Mexico: New Mexico Geological Society, 55th Field Conference, Guidebook, 264-271.

Wallace, A.R., 1995, Cenozoic rift-related sedimentation and faulting, northern Culebra Range, southern Colorado: New Mexico Geological Society, 46th Field Conference, Guidebook, p. 147-154.

Williams, M.L., Karlstrom, K.E., Lanzirotti, A., Read, A.S., Bishop, J.L., Lombardi, C.E., Pedrick, J.N., and Wingsted, M.B., 1999, New Mexico middle-crustal cross sections: 1.65-Ga macroscopic geometry, 1.4-Ga thermal structure, and continued problems in understanding crustal evolution: Rocky Mountain Geology, v. 34, p. 53-66.

Woodward, L.A., 2000, Implications of Jurassic, Cretaceous, and Proterozoic piercing lines for Laramide oblique-slip faulting in New Mexico and rotation of the Colorado Plateau: Discussion and reply: Geological Society of America Bulletin, v. 112, p. 783-785.

Woodward, L.A., Anderson, O.J., and Lucas, S.G., 1999, Late Paleozoic right-slip faults in the ancestral Rocky Mountains: New Mexico Geological Society, 50th Field Conference, Guidebook, p. 149-153.

PLATE 3: ISOSTATIC RESIDUAL GRAVITY – SOUTHERN SAN LUIS BASIN

V.J.S. Grauch and G.R. Keller

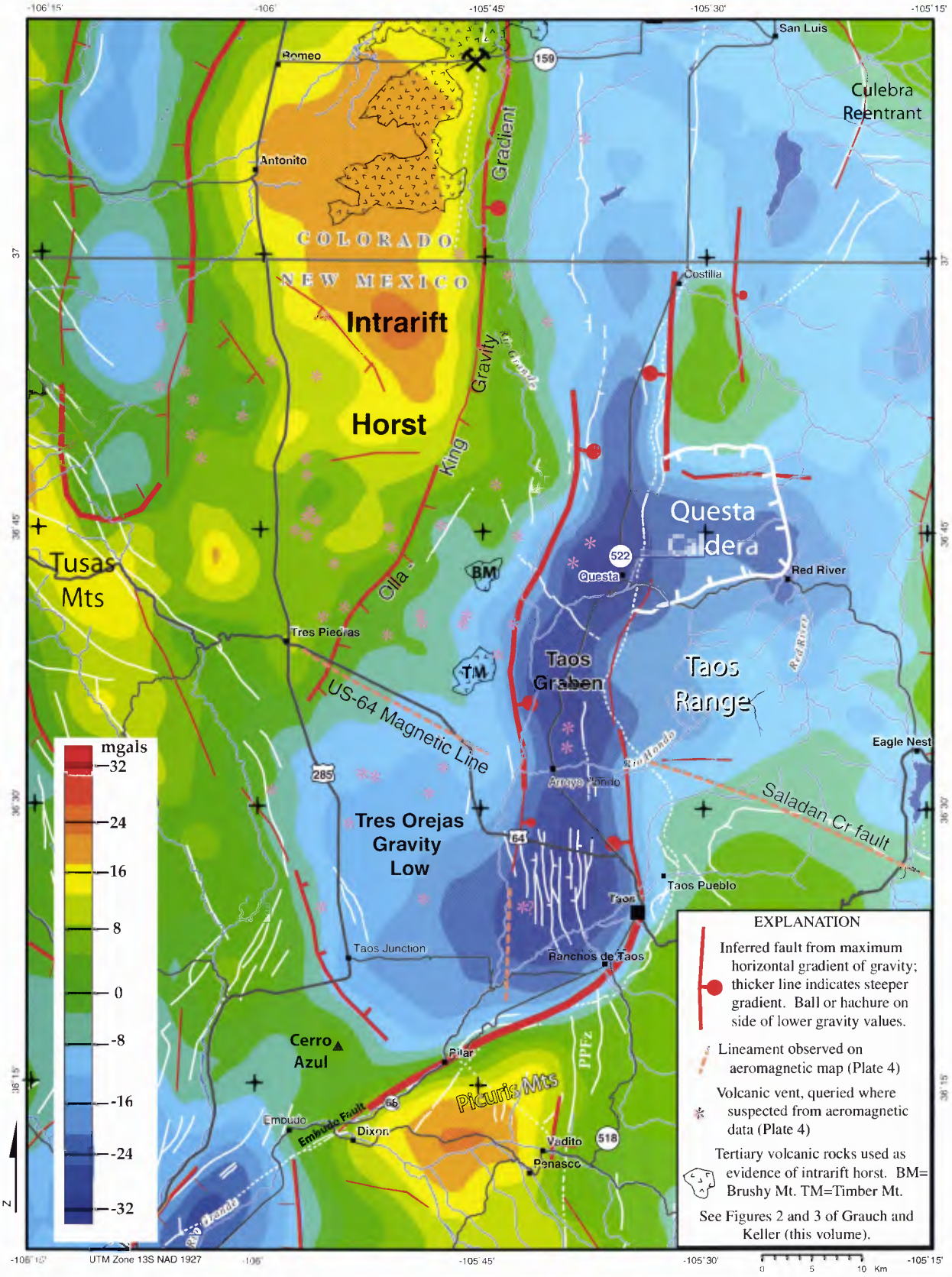


PLATE 3. Color image of isostatic residual gravity data in milligals (mgals) overlain by selected geologic and geophysically interpreted features. Data and interpretations are described in Grauch and Keller (2004 this volume). Mapped faults are shown in white.

PLATE 4: AEROMAGNETIC DATA - SOUTHERN SAN LUIS BASIN

V.J.S GRAUCH AND G.R. KELLER

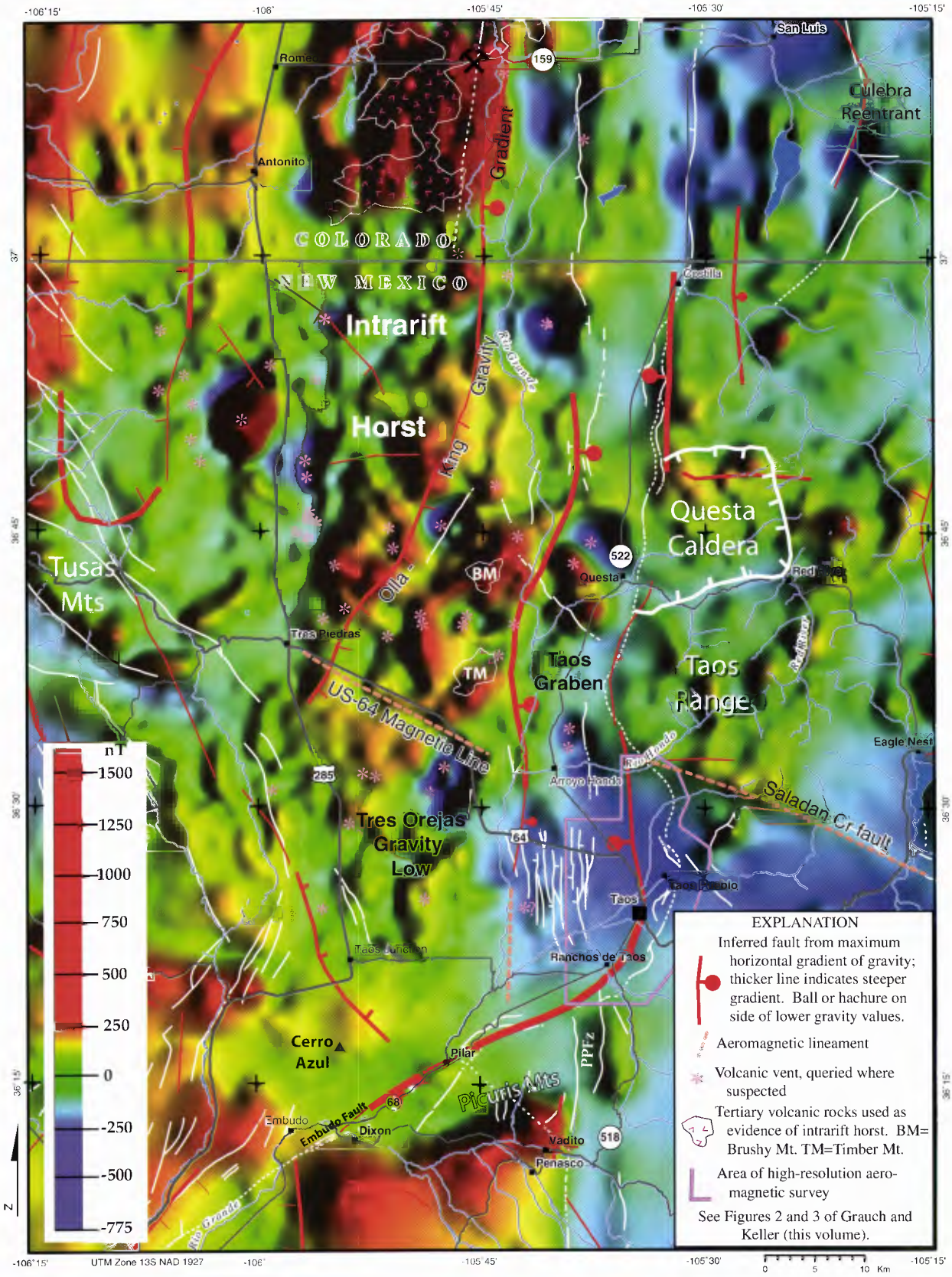


PLATE 4. Color shaded-relief image of reduced-to-pole aeromagnetic data in nanoteslas (nT) overlain by selected geologic and geophysically interpreted features. Data and interpretations are described in Grauch and Keller (2004 this volume). Mapped faults shown in white.